ORIGINAL ARTICLE

Differential Interaction of Metal Ions with Gold Nanoclusters and Application in Detection of Cobalt and Cadmium

Uchangi Satyaprasad Akshath[1,2] · Praveena Bhatt[1,2] ⓘ · Sridevi Annapurna Singh[1,3]

Abstract

Interest in biosensing platforms using protein fluorescent gold nanoclusters (FGNCs) has grown significantly in the past due to the unique optical properties they offer. This study investigates the interaction of metal ions with FGNCs, and the structural modifications brought about by the interaction resulting in fluorescence changes of the cluster and its successful application in the detection of two heavy metals, cobalt and cadmium. The binding of cobalt and cadmium to FGNCs synthesized from BSA significantly altered the secondary structure of the protein, causing a change in its hydrophobicity. It also resulted in a change in fluorescence properties of FGNCs by intersystem crossing (ICT) and fluorescence resonance energy transfer (FRET). Cobalt and cadmium could successfully be detected in the range of 5–165 ng/mL ($R^2 = 0.95$) and 20–1000 ng/ mL ($R^2 = 0.91$), respectively, with appreciable sensitivity. The principle was also applied for the detection of Vitamin B_{12} in commercially available ampoules, validating the proposed method.

Keywords Fluorescent gold nanoclusters · Metal-ion interaction · Circular dichroism · FRET

Introduction

The interaction of metal ions with biomolecules such as proteins have been studied extensively in the past. Protein fluorescent gold nanoclusters (FGNCs) have received significant attention in the field of biosensors due to their ease of synthesis, multiple functional groups for conjugation, and high quantum yield in near-infrared (NIR) window [1, 2]. There are many reports where FGNCs have been successfully synthesized using proteins and have been applied for biosensing and imaging of biomolecules in live cells [3–15]. Interest in FGNPs as optical probes for biosensing has achieved considerable growth due to the protein moiety that can serve as binding sites for numerous analytes. Based on the interaction of protein or gold atom within FGNCs, many groups have successfully designed optical probes for the detection of metal ions [2, 5, 13, 16–19], monitoring enzyme activity [2, 8, 20] and detection of polyphenols [21]. Exploiting the functional groups within the protein, many groups have attempted to use FGNCs as probes for in-vivo imaging in near infra-red range in cancer cells [14, 22–27].

Detection of heavy metals in water is of significant concern due to extensive reports of its contamination in ground and drinking water systems [28–31]. Many groups have successfully used FGNCs for detection of metal ions with reasonable sensitivity in water samples. Liu et al. (2010) reported the detection of cyanide using FGNCs based on cyanide etching triggered fluorescence quenching of FGNCs. A similar approach was used by Xie et al. for mercury detection using gold clusters [32]. Recently, Zhong-Xia Wang et al. developed a turn- off/on the probe using a gold-nickel alloy for detection of mercury and cadmium [33]. Among several proteins, Bovine Serum Albumin (BSA) is extensively used for the synthesis of FGNCs and its application in sensing and imaging. BSA consists of 35 cysteines, 21 tyrosine, 17 histidine, and 2 tryptophan residues that serve to reduce and stabilize gold nanoclusters [34]. It is also well known that serum proteins act as the host for binding of heavy metals and, thus, as

✉ Praveena Bhatt
praveena@cftri.res.in

1 Academy of Scientific and Innovative Research (AcSIR), New Delhi, India

2 Microbiology & Fermentation Technology Department, Central Food Technological Research Institute, Mysore 570020, India

3 Department of Protein Chemistry & Technology, CSIR- Central Food Technological Research Institute (CFTRI), Mysuru 570020, India
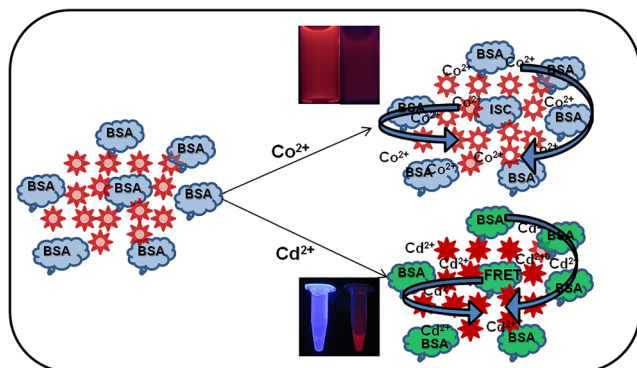
detoxifying agents [35]. To this effect, researchers have reported that cobalt adopts square planar coordination chemistry and binds to N- terminal residue of the protein [36–38]. It is widely believed that the N-terminal residue of BSA serves as binding sites for transition metal ions. Many studies have reported that cadmium exists in complex with biological ligands via chelation [39–41]. The chelation enhanced fluorescence (CEF) mechanism has been utilized by some researchers for detection of cadmium in water/biological fluids [42–45].

To the best of our knowledge, although some reports on detection of metals such as mercury, copper and cyanide [16, 18, 19] using FGNCs have been reported, a clear understanding of the interaction between FGNCs and metal ions leading to fluorescence "turn on" (enhancement of fluorescence) or "off" (fluorescence quenching) is still not established. Interaction between metal ions and FGNCs is often debated for site and mode of interaction [16, 17, 46]. In the present investigation, an attempt was made towards understanding the interaction of cobalt and cadmium with FGNCs. It was hypothesized that the binding of cobalt and cadmium near the vicinity of the clusters changes the secondary structure of the protein as a creation of a hydrophobic environment leading to a change in fluorescence properties of FGNCs. We were able to prove the hypothesis using circular dichroism studies, and the above phenomenon was successfully used for the detection of cobalt and cadmium in water samples. It was also validated using commercial samples containing Vitamin B_{12}, where cobalt is present in the center of the corrin ring (Scheme 1).

Experimental Section

Materials

Bovine serum albumin (BSA), gold chloride trihydrate, vitamin B_{12} and different metal ions were procured from Sigma Chemicals, St. Louis, USA. All reagents used were of analytical grade and acquired from standard suppliers and used without any further purification. For analysis of metal ions in real samples, water was spiked with a known amount of metal ions. For analysis of cobalt, ampoules containing Vit-B_{12} were purchased from drug stores and used after pretreatment.

The instruments used are UV–Vis spectrophotometer (UV-1601, Shimadzu, Japan) for analysis of spectral changes, Spectrofluorimeter (RF-5301 PC, Shimadzu, Japan) for photoluminescence measurements. For Circular dichroism studies, Jasco J-810 spectropolarimeter calibrated with the ammonium salt of d-10-camphor sulfonic acid was used.

Methods

Synthesis of Fluorescent Gold Nanoclusters (FGNCs)

FGNCs were synthesized according to the protocol described by Xie et al. [34]. Briefly, aqueous $HAuCl_4$ solution (5 mL, 10 mM) was added to BSA solution (5 mL, 50 mg/mL) under vigorous stirring. After 2 min, the NaOH solution (0.5 mL, 1 M) was introduced, and the reaction was allowed to proceed under vigorous stirring at 37 °C for 12 h. Both absorption and fluorescence spectra were recorded, and FGNCs were stored at 4 °C until further use.

Studies on the Interaction of Metal Ions with FGNCs

For investigating the interaction of metal ion with FGNCs, various metal ions (Co, Cd, Ba, Na, Fe, Zn, Mn, Mg, and Li) of 100 ng/mL were prepared in phosphate buffer (pH 7.5). Metal ions were incubated with FGNCs for 20 min, and corresponding absorption and fluorescence spectra were recorded.

Circular Dichroism Studies

For investigating the interactions of cobalt and cadmium ions on protein structure, various concentrations of metal ions were prepared (Cobalt- 0.15 and 0.30 μg/mL; cadmium- 0.5 and 1 μg/mL) and incubated with BSA and FGNCs in a separate reaction for 20 min. CD measurements were carried out at 25 °C using a 10 mm path length cell for recording the visible and near UV CD spectra and 1 mm path length cell for far UV CD spectra. Visible and near UV CD spectra were recorded in the range of 290–600 nm with a protein concentration of 3 mg/mL, and far UV CD spectra were recorded in the range 200–260 nm with a protein concentration of 0.4 mg/mL. The mean residue ellipticity [θ] MRW was calculated using a value of 115. Samples were dissolved in PB (7.5). Appropriate blanks were run and deducted from sample runs to correct any extraneous signal. An average of 3 runs at 50 nm/min was considered.

Scheme 1 Depicting the proposed detection method of cadmium and cobalt using FGNCs

Detection of Cobalt & Cadmium by the Proposed Method

For the detection of cobalt and cadmium ions in water samples, the varying concentration of metal ions (Co; 5–165 ng/mL and Cd; 20–1000 ng/ mL) was spiked in water and incubated with FGNCs for 20 min after which, corresponding absorption and fluorescence spectra were recorded. To study the protein structural changes, fluorescence emission at 350 was monitored by exciting FGNCs at 280 nm.

Detection of Vitamin B$_{12}$ by the Proposed Method

For the detection of vit-B$_{12}$ by the proposed method, various concentrations of standard vit-B$_{12}$ were prepared in PB (7.5). To release cobalt from Vit-B$_{12}$, acid extraction method was used as reported previously [47]. After 20 min of incubation of vit-B$_{12}$ with FGNCs, corresponding absorption and fluorescence spectra were recorded. For real sample analysis, ampoules containing vit-B$_{12}$ were purchased from drug stores and processed by acid extraction & dilution-centrifugation method reported previously [47]. Briefly, vit-B$_{12}$ injection ampoules with 0.3 mg/mL were diluted to different concentrations (30, 105 & 120 ng/mL) in PB (7.5), and centrifuged at 10,000 g for 20 min.

Results and Discussion

Synthesis of Fluorescent Gold Nanoclusters

For the synthesis of FGNCs, we adopted previous reports wherein, BSA was used as a sole reducing agent. BSA contains 35 thiol groups from cysteine, which can act as a potential reducing agent for the synthesis of FGNCs [16, 46, 48]. Also, BSA contains 2 tryptophan, 17 histidine, and 21 tyrosine residues that can contribute towards reducing and stabilization of FGNCs [34]. Bright red emission at 620–650 nm was observed under an excitation wavelength of 470 nm. The characteristic absorption and emission spectra of synthesized FGNCs were consistent with earlier reports which confirm the successful synthesis of FGNCs [15].

Studies on the Interaction of Metal Ions with FGNCs

It is well known that structurally BSA can mimic human serum albumin (HSA) which functions as a carrier of a number of metal ions and influences their absorption, transport, metabolism, and detoxification in vivo. Extensive studies of spectroscopic characterizations on the interaction of metal ions and HSA have been reported in literature (Bal et al., 1998; Liu et al., 2009; [33, 35, 38, 49–52]. In the present study, we envisaged the use of FGNCs as nanoprobes for the detection of metal ions exploiting the interaction of BSA with metal ions. As depicted in Fig. 1, the interaction of cobalt (100 ng/mL) with FGNCs quenched the fluorescence of the cluster (80%) whereas, cadmium (100 ng/mL) induced fluorescence enhancement (30%). The other metal ions used in this study, however, did not cause a significant change in fluorescence of FGNCs. These results prompted us to probe the metal-ion cluster interaction further.

Interaction of Cobalt with FGNCs

As presented in Fig. 2, varying concentrations of cobalt ions (5–165 ng/mL) quenched the fluorescence of FGNCs with appreciable linearity ($R^2 = 0.95$). This interaction was observed earlier by Kong Yifei et al. (2013) while conjugating RNase to FGNCs [51]. However, the possible mechanism involved was not investigated by the authors. To understand the phenomenon involved in the quenching process, we performed spectroscopic studies to understand FGNC-metal ion interaction. Results showed (Fig. 3a) that there was an increase in absorbance of the protein upon the interaction of cobalt due to the formation of the metal-ion-ligand complex. This phenomenon, referred to as LMCT (ligand to metal charge transition) has been previously reported by Liang et al. in 2001 [37]. Binding of cobalt to native BSA leads to a sequential change in conformation, causing an increase in the absorbance due to LMCT. In BSA, the Trp 134 residue is located on the surface of the protein and the other (Trp 213) in the hydrophobic pocket [52]. It is the surface Trp, which is responsible for emission at longer wavelengths. As depicted in Fig. 3b, it is evident that the interaction of cobalt with FGNCs led to the appearance of Trp 134 to the surface of the cluster, which emits at a longer wavelength in proportion to cobalt concentration. As depicted in Fig. 3b, at an increasing level of cobalt, there was a marginal decrease in fluorescence of BSA (FGNCs) at 335 nm while at 362 nm, a concentration-dependent increase in fluorescence was observed. These two bands represent the change in the hydrophobic environment as
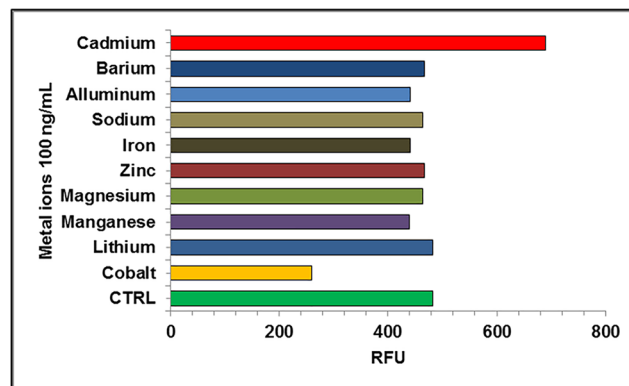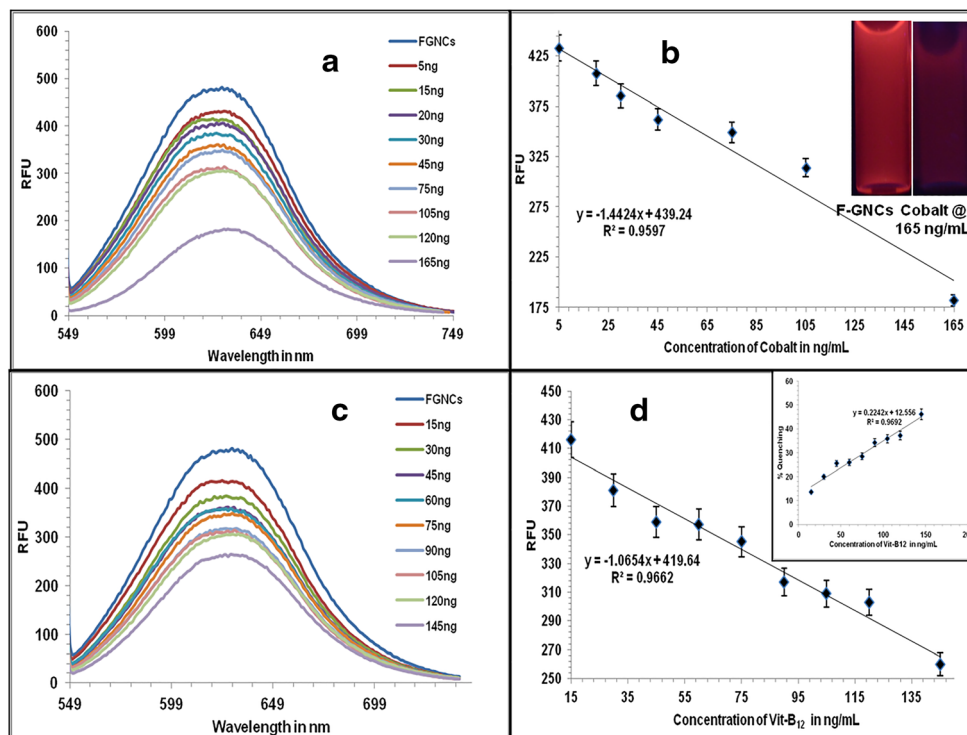

Fig. 1 Interaction of metal ions @ 100 ng/mL with FGNCs

Fig. 2 Interaction of cobalt with FGNCs; (**a**) Varying concentration of cobalt incubated with FGNCs (20 min), (**b**) Standard graph of cobalt with UV image inset (**c**) Fluorescence spectra of Vit-B$_{12}$ interaction with FGNCs (**d**) Standard graph of Vit-B$_{12}$ detection, inset shows the extent of quenching (%)


a function of cobalt concentration. The new band at 362 nm could be due to surface-exposed tryptophan, which was earlier quenched by water molecules and then replaced by cobalt, creating a more hydrophobic environment. Also, at high concentration of cobalt (1 μg/mL) protein (FGNCs) precipitated in solution due to the increase in hydrophobicity (data not shown).

Detection of Vitamin B$_{12}$ by the Proposed Method

Vitamin B$_{12}$ is a cobalt-containing molecule, and its detection has attracted much attention, especially in the field of nutrition and health. As a validation of the concept of using FGNCs as probes for the detection of heavy metals, we used the proposed method to quantitative and detected standard Vit-B$_{12}$

Fig. 3 Spectroscopic studies of cobalt-FGNC interaction; (**a**) Absorbance spectra of FGNCs-cobalt complex (**b**) Changes in protein fluorescence upon FGNC-cobalt interaction (**c**) CD studies depicting changes during FGNC formation and interaction of FGNCs with cobalt
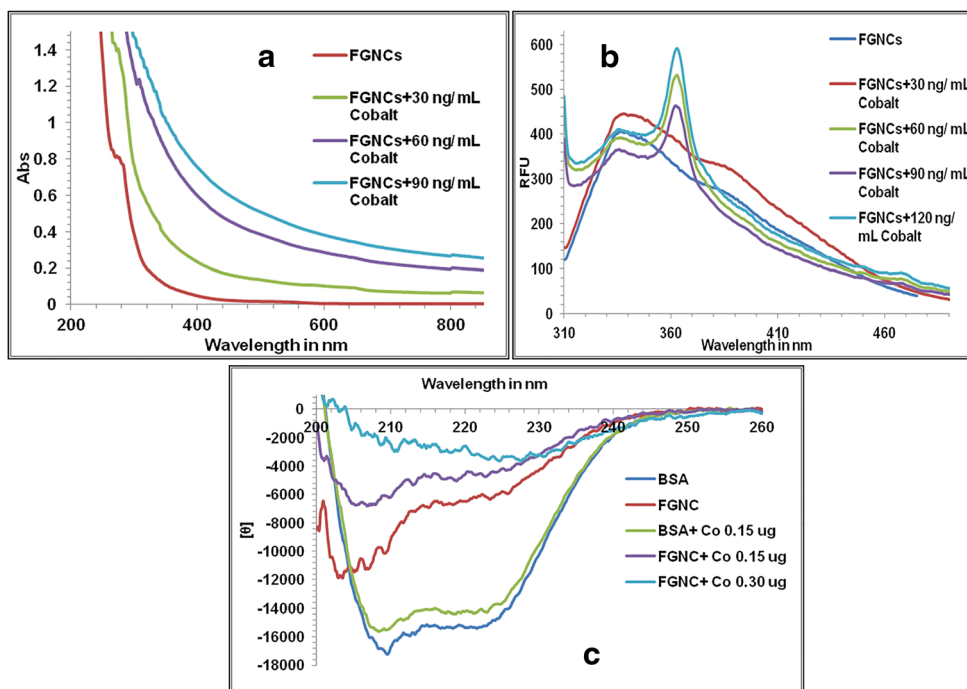
and commercial samples. As depicted in Fig. 1c, d, incubation of varying concentrations of Vit-B$_{12}$ (15–145 ng/mL, LOD 15 ng/mL) with FGNCs for 20 min lead to fluorescence quenching of the clusters ($R^2 = 0.96$). To extend it further, Vit-B$_{12}$ commercially available ampoules were pretreated and extracted for the release of cobalt ion using an earlier reported method [47]. The samples were diluted to the concentration range of the proposed assay (15–145 ng/mL), and analysis was carried out. As depicted in Table 1, good recovery in the samples suggested the application of the proposed method for Vit-B$_{12}$ detection in real samples.

Circular Dichroism (CD) Studies for Co-FGNC Interaction

Circular dichroism (CD) studies were performed to understand the mode of quenching via destabilization of the secondary structure during cluster formation and cobalt interaction. As presented in Fig. 3c, cluster formation affected the secondary structure of native BSA. There were significant changes in the ordered structure of the protein, especially the alpha-helix. BSA is rich in alpha-helix at neutral pH, and a typical spectrum with minima at 222 nm and 208 nm was obtained. As a control, when cobalt (0.30 μg/mL) was added to native BSA, no significant changes in the CD spectrum was observed. However, the formation of FGNCs led to a significant change in the secondary structure of BSA. Figure 3c shows the disappearance of the 222 nm minima and a blue shift of 208 nm minima to 204 nm indicative of unordered structure in the protein. The addition of increasing concentrations of cobalt to FGNCs also led to considerable structural change. This was evident by CD spectra, where we observed an increase in the random structure of BSA (FGNCs) upon interaction with cobalt. This could be due to a change in hydrophobicity of protein upon binding, which was also reflected in the exposure of Trp 134 (domain I). Recently Russell et al., demonstrated by molecular dynamics simulations, that large clusters (~12 atoms) are formed in BSA domain IIB and IA [47]. An extensive study by Liang et al.,

2001 also provides evidence that the binding of cobalt to BSA is concentrated in domain I, which holds large clusters. Due to this reason, the binding of cobalt to FGNCs quenched the fluorescence significantly by ISC (inter-system crossing) phenomenon, which is the hallmark of paramagnetic ions [19].

Interaction of Cadmium with FGNCs

As depicted in Fig. 4, unlike cobalt, the interaction of cadmium with FGNCs led to dose-dependent (20–1000 ng/ mL) "turn-on" fluorescence with good linearity ($R^2 = 0.91$). The fluorescence ratio (I/Io) increased from 1 to 3.34, with more than 300% fluorescence on the binding of cadmium with FGNCs. In order to understand this phenomenon, further studies by spectroscopic methods were carried out. Similar to cobalt, binding of cadmium to FGNCs resulted in an increase of absorbance of FGNCs. This, as discussed, could be due to LMCTs. However, it was observed that Trp fluorescence increased upon the interaction of cadmium with FGNCs (Fig. 5b). This peculiar phenomenon has been previously reported by Wang et al. [32]. The authors concluded that the binding of cadmium to N-terminal amino acids (Lysine) forbids photo-induced electron transfer (PET) phenomenon from nitrogen or oxygen atoms causes an increase in fluorescence. We propose on the basis of absorbance and fluorescence spectra that change in the hydrophobic environment could be responsible for changes in the fluorescence. Also, we observed the turn-on fluorescence of Trp, which can be used as an indicator of protein structural changes [53–55].

Circular Dichroism (CD) Studies for Cd-FGNC Interaction

To delineate the phenomenon, we performed CD experiments using a varying concentration of cadmium. As depicted in Fig. 5c, interactions of FGNCs with cadmium led to a drastic change in secondary structure. The interaction led to the recovery of BSA secondary structure with minima at 222 nm and 208 nm. This observation was indicating the ordered structure formation in the presence of cadmium that was disrupted by FGNCs. Our results are also in agreement with observations of Wang et al. (2016), who performed extensive characterization of the interaction of cadmium with lysozyme and reported that the interaction of cadmium with lysozyme is via hydrophobic means [56].

The case with cadmium is the reverse of what is observed for cobalt interaction with FGNCs. It is reported that the cadmium binding site in BSA is located at the N-terminal residue. It is possible that the chelation of cadmium may have stabilized the secondary structure of BSA in FGNCs, as can be seen from fluorescence and CD spectra. However, the increase of fluorescence of FGNCs as a function of cadmium concentration is due to the FRET phenomenon from Trp to FGNCs. An earlier report on energy transfer from Trp to FGNCs is also available [57].

Table 1 Detection of Vit-B12 in commercial samples against their label and detection of cadmium spiked in water with the proposed method

Sample		
Vitamin B$_{12}$ ampoules 0.3 mg/mL	Vit B$_{12}$ ampoules (ng/mL)*	Quantity detected**
1	30	28.206 ± 1.52
2	105	102.27 ± 0.76
3	120	110 ± 2.93
Cadmium spiked in water	Quantity added in ng/mL	Quantity recovered*
1	20	18.01 ± 1.7
2	100	98 ± 0.65
3	500	499 ± 0.23

*after appropriate dilution; **Average ± SD of Five determinations

Fig. 4 Detection of cadmium by turn-on fluorescence (**a**) Fluorescence spectra of cadmium-FGNC complex (**b**) Standard graph with inset depicts I/Io (**c**) spectral overlap between cadmium bound FGNCs and tryptophan fluorescence
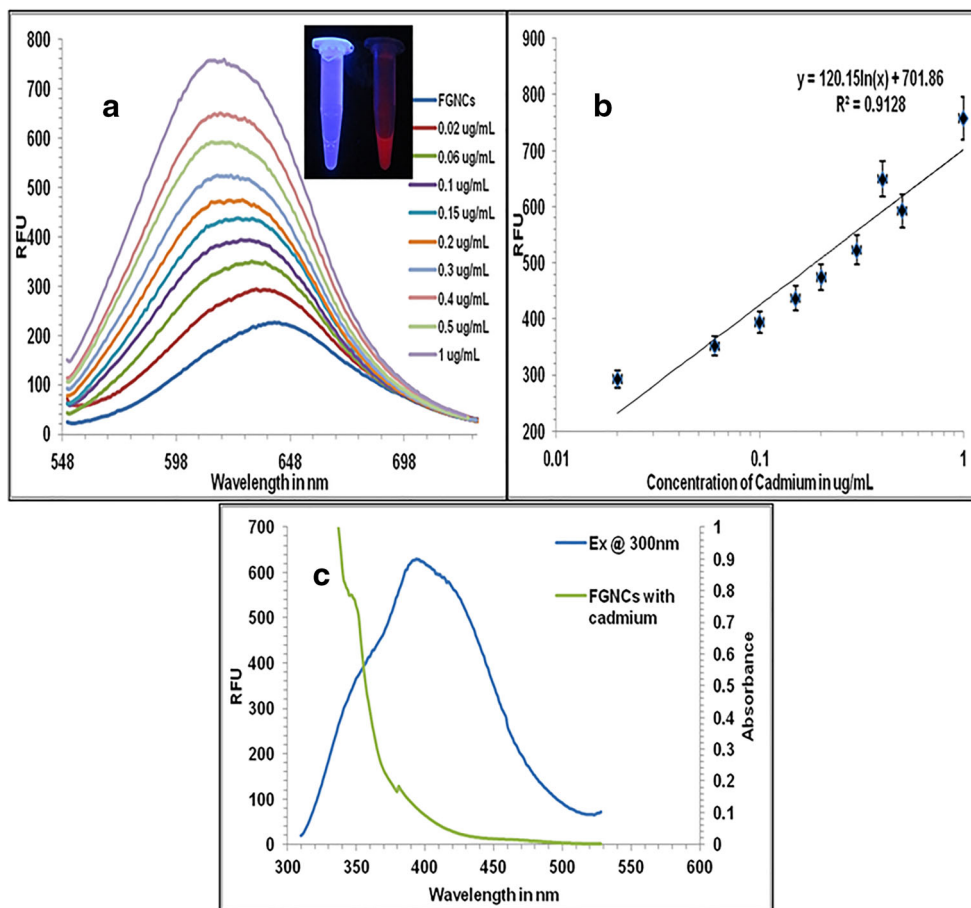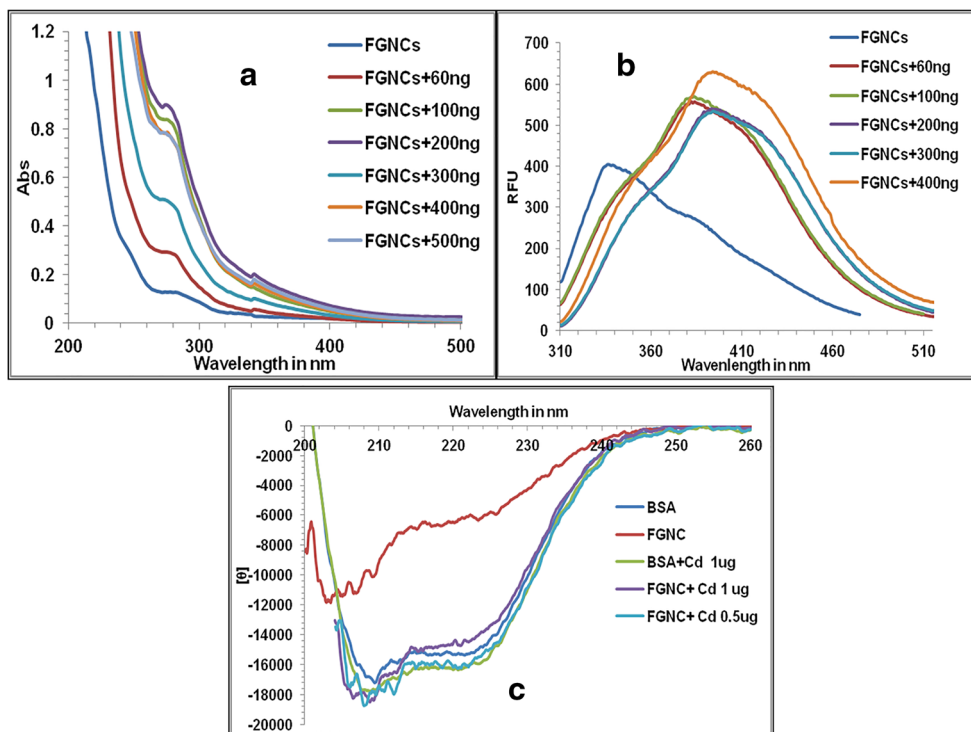

Fig. 5 Spectroscopic studies of cadmium-FGNC interaction (**a**) Absorbance spectra of FGNCs-cadmium complex (**b**) Changes in protein fluorescence upon FGNC-cadmium complex (**c**) CD results of FGNC formation and interaction of FGNC with cadmium

Energy Transfer from Tryptophan to Clusters

There are studies available that show energy transfer from protein to nanoparticles as a result of spectral overlap [57–65]. A good spectral overlap between cadmium bound BSA-clusters and tryptophan fluorescence was observed (Fig. 4c). We report that the synthesis of gold clusters within the BSA core brings the clusters in close proximity with Trp and results in dipolar response interaction between Trp and clusters as a donor-acceptor pair, which results in efficient energy transfer from BSA to clusters. FRET efficiency with respect to varying concentrations of cadmium was calculated using the following equation [58, 62, 66].

$$E = 1 - {^{F_{da}}}/{_{F_d}} \qquad (1)$$

Where F_{da} is the integrated Au-BSA fluorescence in the presence of cadmium and F_d is the integrated Au-BSA fluorescence in the absence of cadmium.

Alternatively, FRET efficiencies can also be calculated using photobleaching rates of the donor in the presence and absence of acceptor. It is widely observed that when resonance energy transfer from donor to acceptor is efficient, it prevents photobleaching of donor and leads to longer photobleaching decay constant. To calculate photobleaching decay time, we used the following equation [58];

$$E = 1 - {^{T_{pb}}}/{_{T'_{pb}}} \qquad (2)$$

Where T_{pb} and T'_{pb} are the photo-bleaching decay time constants of the donor in the presence and absence of the acceptor, respectively. As well known, the time measurements are over seconds rather than nanoseconds which make these measurements easier in comparison with fluorescence lifetime measurements.

Time course fluorescence was monitored for standard BSA, Au-BSA clusters, and Au-BSA clusters with varying
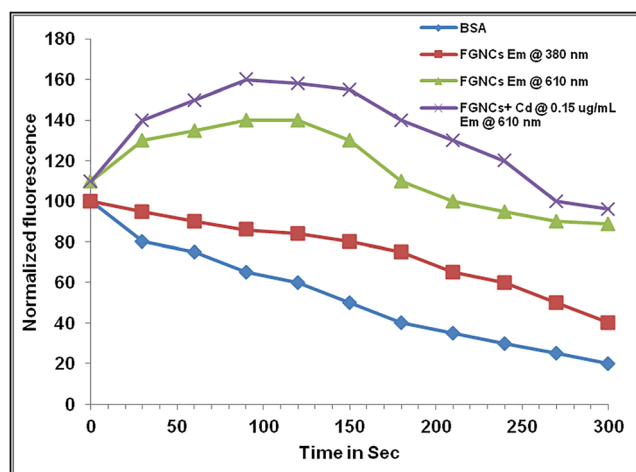

Fig. 6 Studies on photobleaching, emission recorded for BSA @ 350 nm FGNCs @ 380 nm & 610 nm with and without cadmium

Table 2 Photobleaching time & FRET efficiency upon the interaction of cadmium with FGNCs

Sample	Photobleaching time (s)	FRET Efficiency E (%)
FGNCs	70.3	
FGNCs+Cd 0.06 μg/mL	80.5	12.6
FGNCs+Cd 0.15 μg/mL	92.7	24.1
FGNCs+Cd 0.3 μg/mL	107	34.2
FGNCs+Cd 1 μg/mL	125	43.7

cadmium concentrations. Fluorescence measurement was done at 380 nm for the BSA component, whereas, Au-BSA and cadmium-Au-BSA were measured at 610 nm. The energy transfer efficiency was calculated using Eq. 1, and FRET efficiency was calculated using photobleaching theory, which relies on FRET, which will reduce the fluorescence lifetime of the donor molecule by protecting it against photobleaching. As depicted in Fig. 6 and Table 2, the photobleaching time of Au-BSA was reduced in comparison with BSA measured at 380 nm. Whereas, at 610 nm, the photobleaching time of clusters was significantly reduced upon the interaction of cadmium at 0.15 μg/mL. This shows that the energy transfer from tryptophan to clusters upon the interaction of cadmium was the reason for the increase in fluorescence due to efficient FRET. As presented in Table 2, increasing concentration of cadmium led to a decrease in photobleaching time and increased the FRET efficiency from 12.6% to 43.7%. Also, Trp absorbance increased upon interaction with varying concentrations of cadmium with Au-BSA clusters (Fig. 5b). This has led to FRET from tryptophan/tyrosine residues in BSA to clusters, and fluorescence emission drastically increased, leading to the detection of cadmium using Au-BSA clusters.

Conclusion

To conclude, we synthesized FGNCs using BSA as a sole reducing agent that can act as a binding site for the detection of metal ions of our interest. Interaction of various metal ions with FGNCs was studied, and further characterization was performed for cobalt and cadmium ions considering its differential interaction with FGNCs. Spectroscopic investigation revealed that the binding of cobalt and cadmium leads to a change in the hydrophobic environment of FGNCs and drastic changes in the secondary structure of the protein. Further, binding of metal ions in the vicinity of clusters leads to differential interaction of ions with FGNCs that were used for the detection of cobalt, Vit-B$_{12}$, and cadmium at ultrasensitive levels.

References

1. Chen LY, Wang CW, Yuan Z, H.T. (2015) Chang, fluorescent gold nanoclusters: recent advances in sensing and imaging. Anal Chem 87:216–229. https://doi.org/10.1021/ac503636j

2. Chaudhari K, Baksi A, Pradeep T (2012) Protein-protected luminescent noble metal quantum clusters: an emerging trend in atomic cluster nanoscience. Nanotechnol Rev 3:1–16. https://doi.org/10.3402/nano.v3i0.14767

3. Xu Y, Sherwood J, Qin Y, Crowley D, Bonizzoni M, Bao Y (2014) The role of protein characteristics in the formation and fluorescence of Au nanoclusters. Nanoscale. 6:1515–1524. https://doi.org/10.1039/c3nr06040c

4. Chen Y, Wang Y, Wang C, Li W, Zhou H, Jiao H, Lin Q, Yu C (2013) Papain-directed synthesis of luminescent gold nanoclusters and the sensitive detection of Cu^{2+}. J Colloid Interface Sci 396:63–68. https://doi.org/10.1016/j.jcis.2013.01.031

5. Fernández TD, Pearson JR, Leal MP, Torres MJ, Blanca M, Mayorga C, Guével XL (2015) Intracellular accumulation and immunological properties of fluorescent gold nanoclusters in human dendritic cells. Biomaterials. 43:1–12. https://doi.org/10.1016/j.biomaterials.2014.11.045

6. Zhang XD, Wu D, Shen X, Liu PX, Fan FY, Fan SJ (2012) In vivo renal clearance, biodistribution, toxicity of gold nanoclusters. Biomaterials. 33:4628–4638. https://doi.org/10.1016/j.biomaterials.2012.03.020

7. Volden S, Lystvet SM, Halskau Ø, Glomm WR (2012) Generally applicable procedure for in situ formation of fluorescent protein-gold nanoconstructs. RSC Adv:11704–11711. https://doi.org/10.1039/c2ra21931j

8. Wen F, Dong Y, Feng L, Wang S, Zhang S, Zhang X (2011) Horseradish peroxidase functionalized fluorescent gold nanoclusters for hydrogen peroxide sensing. Anal Chem 83:1193–1196. https://doi.org/10.1021/ac1031447

9. Tay CY, Yu Y, Setyawati MI, Xie J, Leong DT (2014) Presentation matters: identity of gold nanocluster capping agent governs intracellular uptake and cell metabolism. Nano Res 7:805–815. https://doi.org/10.1007/s12274-014-0441-z

10. Gao S, Chen D, Li Q, Ye J, Jiang H, Amatore C, Wang X (2014) Near-infrared fluorescence imaging of cancer cells and tumors through specific biosynthesis of silver nanoclusters. Sci Rep 4:4384. https://doi.org/10.1038/srep04384

11. He X, Gao J, Gambhir SS, Cheng Z (2010) Near-infrared fluorescent nanoprobes for cancer molecular imaging: status and challenges. Trends Mol Med 16:574–583. https://doi.org/10.1016/j.molmed.2010.08.006

12. Kawasaki H, Hamaguchi K, Osaka I, Arakawa R (2011) Ph-dependent synthesis of pepsin-mediated gold nanoclusters with blue green and red fluorescent emission. Adv Funct Mater 21:3508–3515. https://doi.org/10.1002/adfm.201100886

13. Liu CL, Wu HT, Hsiao YH, Lai CW, Shih CW, Peng YK et al (2011) Insulin-directed synthesis of fluorescent gold nanoclusters: preservation of insulin bioactivity and versatility in cell imaging. Angew Chem Int Ed 50:7056–7060. https://doi.org/10.1002/anie.201100299

14. Lee H, Lee K, Kim IK, Park TG (2009) Fluorescent gold nanoprobe sensitive to intracellular reactive oxygen species. Adv Funct Mater 19:1884–1890. https://doi.org/10.1002/adfm.200801838

15. Xie J, Zheng Y, Ying JY (2009) Protein-directed synthesis of highly fluorescent gold nanoclusters. J Am Chem Soc 131:888–889. https://doi.org/10.1021/ja806804u

16. Liu Y, Ai K, Cheng X, Huo L, Lu L (2010) Gold-nanocluster-based fluorescent sensors for highly sensitive and selective detection of cyanide in water. Adv Funct Mater 20:951–956. https://doi.org/10.1002/adfm.200902062

17. Zhang L, Wang E (2014) Metal nanoclusters: new fluorescent probes for sensors and bioimaging. Nano Today 9:132–157. https://doi.org/10.1016/j.nantod.2014.02.010

18. Lin Y, Tseng W (2010) Ultrasensitive sensing of Hg^{2+} and CH_3Hg^+ based on the fluorescence quenching of lysozyme type VI-stabilized gold nanoclusters. Anal Chem 82:9194–9200

19. Durgadas CV, Sharma CP, Sreenivasan K (2011) Fluorescent gold clusters as nanosensors for copper ions in live cells. Analyst 136:933–940. https://doi.org/10.1039/c0an00424c

20. Xia X, Long Y, Wang J (2013) Glucose oxidase-functionalized fluorescent gold nanoclusters as probes for glucose. Anal Chim Acta 772:81–86. https://doi.org/10.1016/j.aca.2013.02.025

21. Venkatesh V, Shukla A, Sivakumar S, Verma S (2014) Purine-stabilized green fluorescent gold nanoclusters for cell nuclei imaging applications. ACS Appl Mater Interfaces 6:2185–2191. https://doi.org/10.1021/am405345h

22. Wang Y, Chen J, Irudayaraj J (2011) Nuclear targeting dynamics of gold nanoclusters for enhanced therapy of HER2 + breast cancer. ACS Nano 5:9718–9725. https://doi.org/10.1021/nn2032177

23. Chen L, Wang C, Yuan Z, Chang H (2015) Fluorescent gold nanoclusters: recent advances in sensing and imaging. Anal Chem 87(1):216–229. https://doi.org/10.1021/ac503636j

24. Wang HH, Lin CAJ, Lee CH, Lin YC, Tseng YM, Hsieh CL, Shen JL, Chan WH (2011) Fluorescent gold nanoclusters as a biocompatible marker for in vitro and in vivo tracking of endothelial cells. ACS Nano 5:4337–4344. https://doi.org/10.1021/nn102752a

25. Hu L, Deng L, Alsaiari S, Zhang D, Khashab NM (2014) "Light-on" sensing of antioxidants using gold nanoclusters. Anal Chem 86:4989–4994. https://doi.org/10.1021/ac500528m

26. Hu D, Sheng Z, Fang S, Wang Y, Gao D, Zhang P et al (2014) Folate receptor-targeting gold nanoclusters as fluorescence enzyme mimetic nanoprobes for tumor molecular colocalization diagnosis. Theranostics 4:142–153. https://doi.org/10.7150/thno.7266

27. Cho SJ, Maysinger D, Jain M, Röder B, Hackbarth S, Winnik FM (2007) Long-term exposure to CdTe quantum dots causes functional impairments in live cells. Langmuir 23:1974–1980. https://doi.org/10.1021/la060093j

28. Pan J, Plant JA, Voulvoulis N, Oates CJ, Ihlenfeld C (2010) Cadmium levels in Europe: implications for human health. Environ Geochem Health 32:1–12. https://doi.org/10.1007/s10653-009-9273-2

29. S.I. Report, Cadmium risks to freshwater life : derivation and validation of low-effect criteria values using laboratory and field studies scientific investigations report 2006–5245, Quality. (2010)

30. Godt J, Scheidig F, Grosse-Siestrup C, Esche V, Brandenburg P, Reich A, Groneberg DA (2006) The toxicity of cadmium and resulting hazards for human health. J Occup Med Toxicol 1:22. https://doi.org/10.1186/1745-6673-1-22

31. Xie J, Zheng Y, Ying JY (2010) Highly selective and ultrasensitive detection of Hg(2+) based on fluorescence quenching of Au nanoclusters by Hg(2+)-Au(+) interactions. Chem Commun (Camb) 46:961–963. https://doi.org/10.1039/b920748a

32. Wang ZX, Guo YX, Ding SN (2015) Fluorometric determination of cadmium (II) and mercury(II) using nanoclusters consisting of a gold-nickel alloy. Microchim Acta 182:2223–2231. https://doi.org/10.1007/s00604-015-1563-z

33. Bal W, Christodoulou J, Sadler PJ, Tucker A (1998) Multi-metal binding site of serum albumin. J Inorg Biochem 70:33–39. https://doi.org/10.1016/S0162-0134(98)00010-5

34. Wei H, Wang Z, Yang L, Tian S, Hou C, Lu Y (2010) Lysozyme-stabilized gold fluorescent cluster: synthesis and application as Hg(2+) sensor. Analyst. 135:1406–1410. https://doi.org/10.1039/c0an00046a

35. Liu H, Xu Z, Liu X, Xi P, Zeng Z (2009) Analysis of binding interaction between bovine serum albumin and the cobalt (II) complex with salicylaldehyde-2-phenylquinoline-4-carboylhydrazone. Chem Pharm Bull (Tokyo) 57:1237–1242. https://doi.org/10.1248/cpb.57.1237

36. Sokołowska M, Wszelaka-Rylik M, Poznański J, Bal W (2009) Spectroscopic and thermodynamic determination of three distinct binding sites for Co (II) ions in human serum albumin. J Inorg Biochem 103:1005–1013. https://doi.org/10.1016/j.jinorgbio.2009.04.011

37. Liang H, Huang J, Tu C, Zhang M, Zhou Y, Shen P (2001) The subsequent effect of interaction between Co 2 1 and human serum albumin or bovine serum albumin. J Inorg Biochem 85:167–171

38. Qu SS, Liu Y, Wang TZ, Gao WY (2002) Thermodynamics of binding of cadmium to bovine serum albumin. Chemosphere. 46:1211–1214. https://doi.org/10.1016/S0045-6535(01)00213-2

39. Andersen O (1983) Chelation of cadmium. Environ Health Perspect 54:249–266. https://doi.org/10.1289/ehp.8454249

40. Martins E, Drakenberg T (1982) Cadmium (II), Zinc (II), and Copper (II) ions binding to bovine serum albumin. A 113Cd NMR study. Inorg Chim Acta 67:71–74

41. Cheng T, Xu Y, Zhang S, Zhu W, Qian X, Duan L (2008) A highly sensitive and selective OFF-ON fluorescent sensor for cadmium in aqueous solution and living cell. J Am Chem Soc 130:16160–16161. https://doi.org/10.1021/ja806928n

42. Williams NJ, Gan W, Reibenspies JH, Hancock RD (2009) Possible steric control of the relative strength of chelation enhanced fluorescence for zinc (II) compared to cadmium (II): metal ion complexing properties of tris(2-quinolylmethyl) amine, a crystallographic, UV-visible, and fluorometric study. Inorg Chem 48:1407–1415. https://doi.org/10.1021/ic801403s

43. Peng X, Du J, Fan J, Wang J, Wu Y, Zhao J et al (2007) A selective fluorescent sensor for imaging Cd^{2+} in living cells. J Am Chem Soc 129:1500–1501. https://doi.org/10.1021/ja0643319

44. Yang Y, Cheng T, Zhu W, Xu Y, Qian X (2011) Highly selective and sensitive near-infrared fluorescent sensors for cadmium in aqueous solution. Org Lett 13:264–267. https://doi.org/10.1021/ol102692p

45. Huang C-C, Yang Z, Lee K-H, Chang H-T (2007) Synthesis of highly fluorescent gold nanoparticles for sensing mercury (II). Angew Chem 119:6948–6952. https://doi.org/10.1002/ange.200700803

46. Wei H, Wang Z, Zhang J, House S, Gao Y-G, Yang L, Robinson H, Tan LH, Xing H, Hou C, Robertson IM (2011) Time-dependent, protein-directed growth of gold nanoparticles within a single crystal of lysozyme. Nat Nanotechnol 6:93–97. https://doi.org/10.1038/nnano.2010.280

47. Russell BA, Kubiak-Ossowska K, Mulheran PA, Birch DJS, Chen Y (2015) Locating the nucleation sites for protein encapsulated gold nanoclusters: a molecular dynamics and fluorescence study. Phys Chem Chem Phys 17:21935–21941. https://doi.org/10.1039/c5cp02380g

48. Li J, Zhu JJ, Xu K (2014) Fluorescent metal nanoclusters: from synthesis to applications. TrAC - Trends Anal Chem 58:90–98. https://doi.org/10.1016/j.trac.2014.02.011

49. Sadler PJ, Tucker A, Viles JH (1994) Involvement of a lysine residue in the N-terminal Ni^{2+} and Cu^{2+} binding site of serum albumins. Comparison with Co^{2+}, Cd^{2+} and Al^{3+}. Eur J Biochem 220:193–200. https://doi.org/10.1111/j.1432-1033.1994.tb18614.x

50. Zhang YZ, Li HR, Dai J, Chen WJ, Zhang J, Liu Y (2010) Spectroscopic studies on the binding of cobalt (II) 1,10-Phenanthroline complex to bovine serum albumin. Biol Trace Elem Res 135:136–152. https://doi.org/10.1007/s12011-009-8502-y

51. Yifei K, Chen J, Gao F, Brydson R, Johnson B, Heath G, Zhang Y, Wu L, Zhou D (2013) Near-infrared fluorescent ribonuclease-A-encapsulated gold nanoclusters: preparation, characterization, cancer targeting and imaging. Nanoscale 5(3):1009–1017. https://doi.org/10.1039/C2NR32760K

52. Moriyama Y, Ohta D, Hachiya K, Mitsui Y, Takeda K (1996) Fluorescence behavior of tryptophan residues of bovine and human serum albumins in ionic surfactant solutions: a comparative study of the two and one tryptophan(s) of bovine and human albumins. J Protein Chem 15:265–272. https://doi.org/10.1007/BF01887115

53. Ghisaidoobe ABT, Chung SJ (2014) Intrinsic tryptophan fluorescence in the detection and analysis of proteins: a focus on förster resonance energy transfer techniques. Int J Mol Sci 15:22518–22538. https://doi.org/10.3390/ijms151222518

54. Vivian JT, Callis PR (2001) Mechanisms of tryptophan fluorescence shifts in proteins. Biophys J 80:2093–2109. https://doi.org/10.1016/S0006-3495(01)76183-8

55. Hospes M, Hendriks J, Hellingwerf KJ (2013) Tryptophan fluorescence as a reporter for structural changes in photoactive yellow protein elicited by photo-activation. Photochem Photobiol Sci 12:479–488. https://doi.org/10.1039/C2PP25222H

56. Wang J, Yang X, Wang J, Xu C, Zhang W, Liu R, Zong W (2016) Probing the binding interaction between cadmium (II) chloride and lysozyme. New J Chem 40(4):3738–3746

57. Raut S, Chib R, Butler S, Borejdo J, Gryczynski Z, Gryczynski I (2014) Evidence of energy transfer from tryptophan to BSA/HSA protected gold nanoclusters. Methods Appl Fluores 2:35004. https://doi.org/10.1088/2050-6120/2/3/035004

58. Vinayaka AC, Thakur MS (2011) Photoabsorption and resonance energy transfer phenomenon in CdTe-protein bioconjugates: an insight into QD-biomolecular interactions. Bioconjug Chem 22:968–975. https://doi.org/10.1021/bc200034a

59. Medintz IL, Mattoussi H (2009) Quantum dot-based resonance energy transfer and its growing application in biology. Phys Chem Chem Phys 11:17–45. https://doi.org/10.1039/b813919a

60. Medintz IL, Clapp AR, Mattoussi H, Goldman ER, Fisher B, Mauro JM (2003) Self-assembled nanoscale biosensors based on quantum dot FRET donors. Nat Mater 2:630–638. https://doi.org/10.1038/nmat961

61. Chong EZ, Matthews DR, Summers HD, Njoh KL, Errington RJ, Smith PJ (2007) Development of FRET-based assays in the far-red using CdTe quantum dots. Biomed Res Int. https://doi.org/10.1155/2007/54169

62. Patel RC, Lange DC, Patel YC (2002) Photobleaching fluorescence resonance energy transfer reveals ligand-induced oligomer formation of human somatostatin receptor subtypes. Methods. 27:340–348. https://doi.org/10.1016/S1046-2023(02)00092-0

63. Wang S, Liu P, Qin Y, Chen Z, Shen J (2016) Rapid synthesis of protein conjugated gold nanoclusters and their application in tea polyphenol sensing. Sensors Actuators B Chem 223:178–185. https://doi.org/10.1016/j.snb.2015.09.058

64. Dieaconu M, Loanid A, Iftimie S, Antohe S (2012) UV-absorption mechanisms of Ni^{2+}-binding bovine serum albumin. Dig J Nanomater Biostruct 7:1125–1137

65. Shaw AK, Pal SK (2008) Spectroscopic studies on the effect of temperature on pH-induced folded states of human serum albumin. J Photochem Photobiol B Biol 90:69–77. https://doi.org/10.1016/j.jphotobiol.2007.11.003

66. Selvakumar LS, Ragavan KV, Abhijith KS, Thakur MS (2013) Immunodipstick based gold nanosensor for vitamin B12 in fruit and energy drinks. Anal Methods 5:1806. https://doi.org/10.1039/c3ay26320g